Liquid Crystals
Publication details, including instructions for authors and subscription information:
http://www.informaworld.com/smpp/title~content=t713926090

Giant surface electroclinic effect in a chiral smectic A liquid crystal

Ren-Fan Shao[a]; Joseph E. MacLennan[a]; Noel A. Clark[a]; Daniel J. Dyer[b]; David M. Walba[b]
[a] Department of Physics and Ferroelectric Liquid Crystal Materials Research Center, University of Colorado, Boulder CO 80309, USA, [b] Department of Chemistry and Biochemistry and Ferroelectric Liquid Crystal Materials Research Center, University of Colorado, Boulder CO 80309, USA,

Online publication date: 06 August 2010

To cite this Article Shao, Ren-Fan , MacLennan, Joseph E. , Clark, Noel A. , Dyer, Daniel J. and Walba, David M.(2001) 'Giant surface electroclinic effect in a chiral smectic A liquid crystal', Liquid Crystals, 28: 1, 117 — 123
To link to this Article: DOI: 10.1080/026782901462454
URL: http://dx.doi.org/10.1080/026782901462454

LIQUID CRYSTALS, 2001, VOL. 28, NO. 1, 117–123

Giant surface electroclinic effect in a chiral smectic A liquid crystal

REN-FAN SHAO, JOSEPH E. MACLENNAN*, NOEL A. CLARK
Department of Physics and Ferroelectric Liquid Crystal Materials Research Center, University of Colorado, Boulder CO 80309, USA

DANIEL J. DYER and DAVID M. WALBA
Department of Chemistry and Biochemistry and Ferroelectric Liquid Crystal Materials Research Center, University of Colorado, Boulder CO 80309, USA

(*Received 13 March 2000; accepted 19 May 2000*)

We report the observation of a very large surface electroclinic effect in the smectic A* phase of a chiral liquid crystal. In planar-aligned cells of enantiomerically pure W415, the smectic A* phase grows in from the isotropic state with the layer normal rotated $\psi = -24°$ from the rubbing direction, a consequence of the surface electroclinic tilt θ_s of the director. The sign of θ_s depends on the molecular handedness, with $\theta_s \equiv 0$ in the racemate, and increasing linearly with moderate enantiomeric excess before saturating as $ee \to 1$. A uniform layer structure can be achieved using cross-rubbed alignment layers, in which case thin cells of W415 in the smectic C* phase display V-shaped (analogue) electro-optic switching.

1. Introduction

Understanding the interaction of liquid crystals (LCs) with rubbed polymer surfaces is central to controlling the bulk alignment, and hence the electro-optic properties of LC cells. When the smectic A (SmA) phase of an achiral liquid crystal appears from the isotropic or nematic phase in a cell that is rubbed to induce parallel (homogeneous) alignment of the molecules, the smectic layers form with their layer normal $\hat{z}$ along the rubbing direction $\hat{R}$, the direction favoured by the molecules. In chiral materials, however, $\hat{z}$ typically makes a finite angle ψ with the rubbing direction [1]. When ψ is larger than a few degrees, the overall alignment in parallel-rubbed cells becomes very poor because the layers in the top and bottom halves of the cell grow in with noticeably different orientations, and the electro-optic properties in the smectic C* (SmC*) phase are correspondingly degraded.

In order to achieve good alignment in surface-stabilized ferroelectric liquid crystal (SSFLC) cells [2], it is essential to understand the physical mechanism of the surface-induced director rotation. Xue and Clark have proposed [3] that a surface electroclinic effect accounts for the angular deviation of the SmA* layer normal from the rubbing direction, the liquid crystal essentially undergoing a phase transition to the SmC* at the surface of the cell, where the director is tilted by θ_s. At the isotropic–SmA* transition, the liquid crystal molecules align preferentially along the rubbing direction and the layers are uniformly rotated so that at the surface the director lies on the induced tilt cone. The layer orientation is maintained into the interior of the cell, even though the LC relaxes back into the SmA* phase, the induced tilt becoming rapidly smaller with distance from the cell surface until $\theta = 0$. This model, rather than an alternative mechanism suggested by Patel *et al.* [4], has been confirmed independently by Chen *et al.* [5]. A surface electroclinic effect has also been observed in chiral nematics [6, 7].

In this paper we report the observation of the largest known surface electroclinic effect in the SmA* phase, in the chiral compound W415. The rotation of the layer normal from the rubbing direction reaches $\psi = 24°$, a value that is appreciably larger than anything previously observed [1, 3–5, 8]. Cross-rubbing is used to produce cells with uniform layering, as well as samples where the layers growing in from the two surfaces are twisted by 90°. Textural studies suggest the existence of a new kind of focal-conic defect, and allow us to map the topography of the twisted layer boundaries that form between the top and bottom sets of layers.

*Author for correspondence; e-mail: jem@colorado.edu

Liquid Crystals ISSN 0267-8292 print/ISSN 1366-5855 online © 2001 Taylor & Francis Ltd
http://www.tandf.co.uk/journals

2. Experimental

W415 has the structure shown in figure 1 and the following bulk phase sequence:

$$\text{Isotropic} \xleftrightarrow{34.3^{\circ}\text{C}} \text{SmA*} \xleftrightarrow{24.1^{\circ}\text{C}} \text{SmC*} \xleftrightarrow{<0^{\circ}\text{C}} \text{Crystal.}$$

ITO-glass cells 2 μm thick prepared with (rubbed) nylon alignment layers are filled by capillarity in the isotropic phase, then cooled slowly (at $-0.1^{\circ}\text{C min}^{-1}$) into the SmA* phase. In general, the smectic layers nucleate first at the two cell surfaces. In cells with only one plate rubbed, the layers nucleate first at the rubbed surface, then grow across the cell until they reach the non-rubbed plate, which implies that rubbing induces additional order, effectively raising the isotropic–smectic transition temperature. The onset of smectic ordering in such a cell is illustrated in figure 2 (*a*). The dark horizontal lines in this image are macroscopic scratches left by the rubbing brush, that apparently help to nucleate layer formation. The other lines in the weakly birefringent smectic texture are parallel to the layer normal, which is seen to be rotated counter-clockwise from the rubbing direction. The magnitude of this deviation does not change once the layers are formed at the isotropic–SmA* transition, i.e. ψ is constant over the entire SmA*–SmC* temperature range.

It is conventional to define the sign of ψ as positive when the layer normal $\hat{z}$ at the bottom plate of the cell is rotated clockwise from the rubbing direction $\hat{R}$ when viewed from above, see figure 2 (*b*). Equivalently, when the director $\hat{n}$ (along the rubbing) is offset counter-clockwise from the layer normal (the usual convention for a positive rotation) then $\psi > 0$. In general, the sign of surface tilt is that of $(\hat{z} \times \hat{n})\ \hat{s}$, where $\hat{s}$ is the surface normal pointing from the glass into the LC.

In order to gain insight into what determines θ_s, and hence the magnitude of the smectic layer rotation ψ, we have compared measurements of the bulk and surface electroclinic tilts, and examined the spontaneous polarization in the SmC* phase. The magnitudes of the induced surface tilt θ_s in the SmA* phase, and of the saturated spontaneous polarization P in the SmC* phase (at 8°C), were determined for W415 (*S*), its enantiomer W434 (*R*), and their racemic mixture (W435) in the same type of cell. We find that the sign of θ_s is correlated with that of P, so that $\hat{P}$ always points into the liquid crystal at the cell surfaces, i.e. $\hat{P} \parallel \hat{s}$ (see the table).

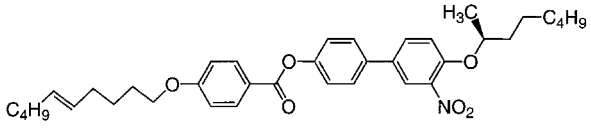

Figure 1. Chemical structure of W415.

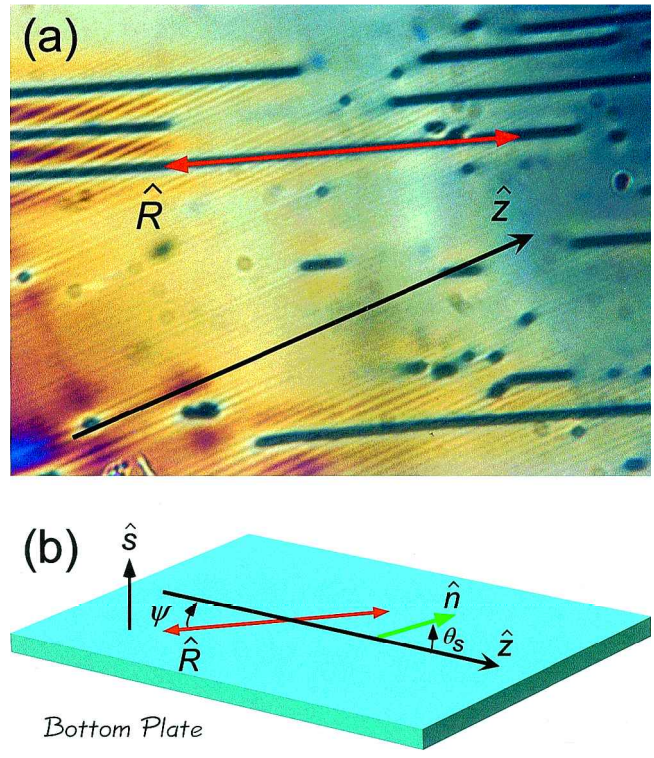

Figure 2. (*a*) Polarized photomicrograph showing smectic layer formation at the isotropic–SmA* transition in a typical W415 cell ($d \sim 3.5$ μm) rubbed on the bottom surface only. The layer normal $\hat{z}$ is rotated from the direction of rubbing $\hat{R}$, defined by the dark scatches left in the nylon alignment layer. By definition the layer rotation ψ in this material is negative. The horizontal dimension is about 200 μm. (*b*) Layer rotation sign convention: a positive rotation ψ obtains when $\hat{z} \times \hat{n} \parallel \hat{s}$, the glass surface normal. In general, $\hat{n}$ is along $\hat{R}$ when the smectic layers initially form, but deviates from this direction on further cooling.

Table. Saturated smectic C* spontaneous polarization and surface electroclinic tilt of compounds in the W415 family. The data were obtained in $d \sim 2$ μm cells with nylon alignment layers rubbed on one surface only.

Material	Chirality	P/nC cm^{-2}	θ_s/°
W415	*S*	− 340	− 24
W434	*R*	+ 338	+ 24
W435	racemic	0	0

We also investigated the relationship between θ_s and P quantitively, studying a series of mixtures of W415 or W434 in the racemate, increasing the relative amount of the respective enantiomer in steps of 20% by weight in each new mixture. As shown for W434 in figure 3 (*a*), the induced surface tilt varies linearly for small enantiomeric excesses, and becomes increasingly non-linear as ee → 1.

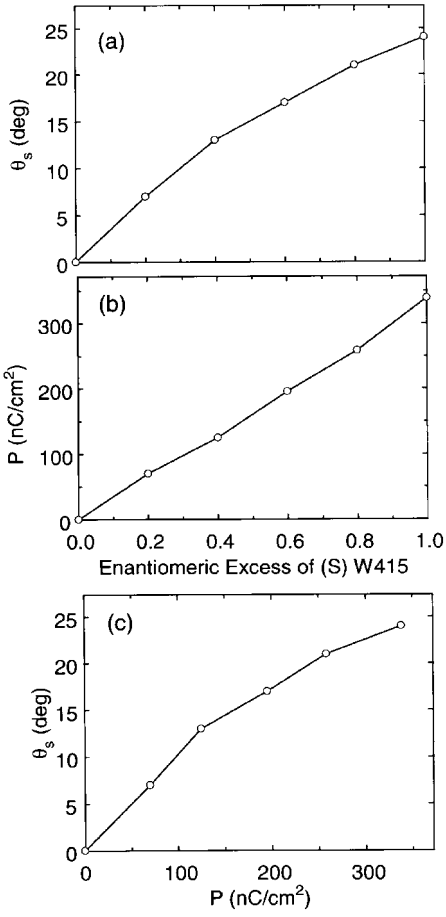

Figure 3. Measured dependence of (*a*) θ_s and (*b*) P on enantiomeric excess ee in W415 mixtures. The linearity of the polarization data in (*b*) results in a θ_s vs. P plot (*c*) which resembles the curve in (*a*).

The bulk polarization P varies linearly with ee, as is typical in chiral smectic C mixtures, figure 3 (*b*). Since $P \propto$ ee, the θ_S vs. P plot in figure 3 (*c*) has qualitatively the same shape as in 3 (*a*). The behaviour of the W415 mixtures is identical, except that the signs of both θ_S and P are negative.

For comparison purposes, we measured the magnitude of the bulk electroclinic rotation θ_B as a function of applied electric field, for both W415 and W434. As shown in figure 4, the response is large and the form of $\theta_B(E)$ is similar to that of $\theta_S(P)$ in the surface electroclinic effect, figure 3 (*c*). The saturation bulk electroclinic tilt is 23°, essentially the same value as the surface electroclinic tilt in the pure enantiomer (but smaller than the saturated SmC tilt $\theta \sim 30.5°$ at 8°C).

3. Layer alignment by rubbing

We now describe the effects of rubbing on the alignment. In cells prepared with both plates rubbed parallel, the different surface director tilts induced by the surface

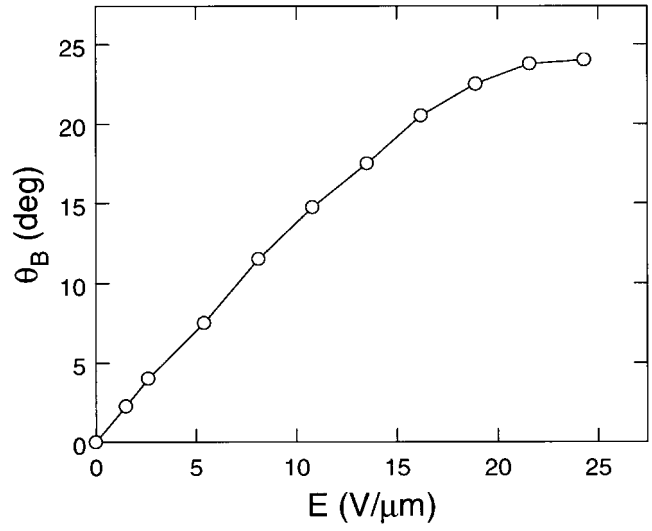

Figure 4. Bulk electroclinic tilt response $\theta_B(E)$ of W415 at 30°C.

electroclinic effect prevent a uniform alignment of the director field. On cooling slowly from the isotropic phase, smectic layers nucleate independently at both plates, grow in towards the middle of the cell, and eventually connect. Figure 5 (*a*) shows the typical texture of such a cell. The two sets of parallel lines rotated by $2\psi \approx 48°$ reveal the layer normal orientations in the upper and lower halves of this cell. In most parts of the cell, the upper and lower sets of layers meet approximately in the middle, producing the average pink–yellow birefringence colour seen in much of the photograph. The anomalous blue regions are places where one layer orientation penetrates through most of the thickness of the cell, yielding a slightly higher effective birefringence. This localized SmA texture necessarily implies a new kind of focal-conic defect, the detailed structure of which we do not completely understand, but which is sketched roughly in figure 5 (*b*). Thick ($d \gtrsim 5\,\mu$m) cells which are cooled rapidly are filled with these focal-conic defects, as shown in figure 5 (*c*).

For liquid crystals with a big surface electroclinic effect, good alignment can reliably be achieved only using crossed (non-parallel) rubbing as illustrated in figure 6: after rubbing both plates (*a*), the top plate is flipped over (*b*) and rotated through $2\theta_s$, then placed on the bottom plate. When the rotation is negative (*c*) the layers grow in with a uniform orientation throughout the cell (*d*); if it is positive (*e*) and $4\theta_s \approx 90°$ (as in the case of W434), then the layer normals become approximately perpendicular (*f*).

In cross-rubbed cells of W415 with uniform layering, we observe classical 'V-shaped' switching (an electro-optic response symmetric about $E = 0$ that is linear over a wide voltage range before saturating) in the SmC* phase (see figure 7). The surface electroclinic effect stabilizes a

'twisted' director field in the cell and provides strong polar anchoring at the surfaces [9, 10].

When a W415 cell is assembled with the layer normals approximately perpendicular, the birefringences in the upper and lower parts of the cell in the SmA* phase effectively have opposite signs. When the layers meet precisely in the middle of the cell, the birefringence cancels indentically and the liquid crystal appears black between crossed polarizers, irrespective of the cell orientation, giving a characteristic texture of dark brushes such as those in figure 8 (*a*). The position of the layer twist interface varies in the cell, giving different birefringence colours, as shown in figure 8 (*b*) and modified by a phase compensator in figures 8 (*c*)–(*e*). The fluctuations in interface position, sketched qualitatively in figure 8 (*f*), are surprisingly large, extending to both surfaces of the cell.

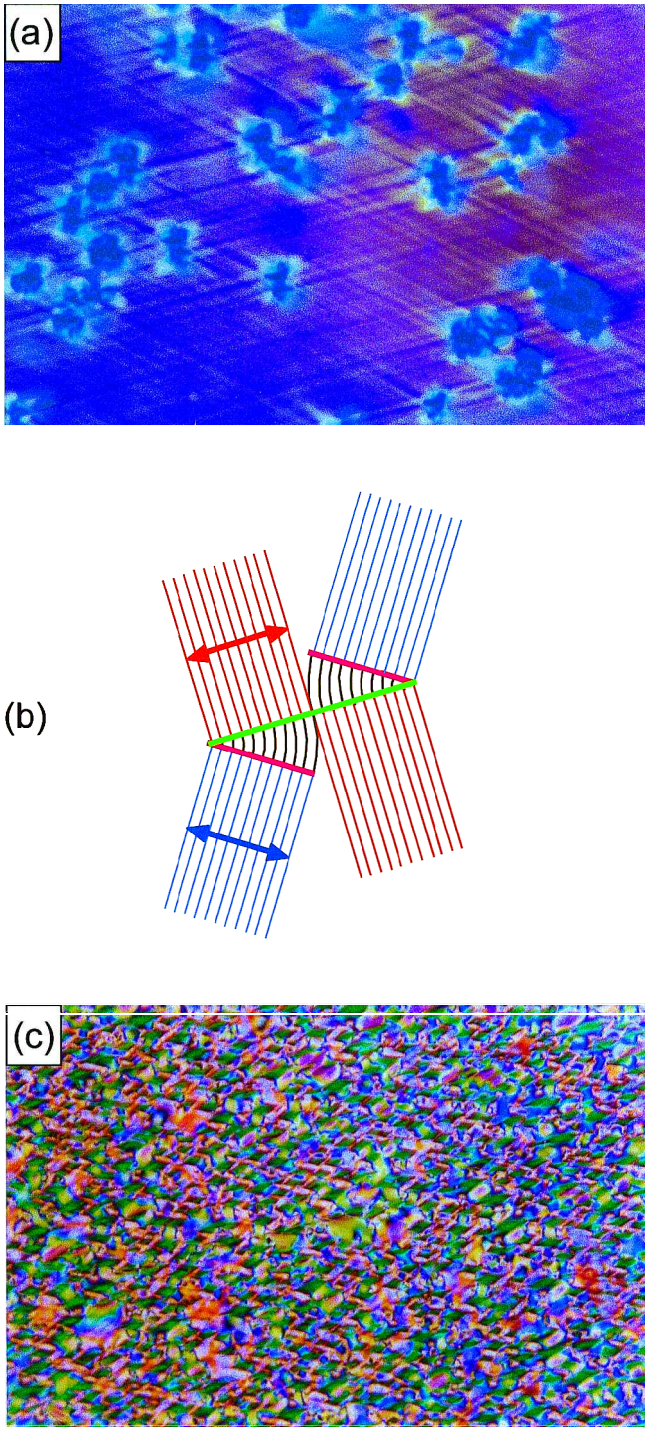

Figure 5. Textures and layer structure of parallel-rubbed cells of W415. (*a*) In a 2 μm cell the texture is quite uniform, indicating planar alignment of the director and a smooth interface between the upper and lower layers, with the exception of characteristic localized defects (blue domains) which typically have either left- or right-handed pinwheel symmetry. The layer normals in the upper and lower parts of the cell are crossed at an angle $2\psi \approx 48°$. (*b*) Schematic of the layer structure near the localized defects shown in (*a*). The red and blue lines represent the layers in the upper and lower regions, respectively, with the layer normals (indicated by the heavy arrows) parallel to the texture striations in (*a*). The black curved layers represent a focal-conic-like connection between the upper and lower layers, which must penetrate into both the red and blue layers, perhaps going from glass plate to glass plate. How the blue (red) layers would connect with the black along the magenta (green) lines is unclear. (*c*) Focal-conic texture of a thick ($d \sim 5$ μm) cell. The horizontal dimensions of (*a*) and (*c*) are about 200 μm.

4. Theoretical model

To describe the surface electroclinic effect theoretically, we use Landau formalism [3, 8, 11, 12], writing the bulk free energy density of the SmA* phase in terms of the polarization P and tilt angle θ as

$$F = F_A + \frac{1}{2}A'\theta^2 + \frac{1}{4}B\theta^4 + \frac{1}{2\chi}P^2 - tP\theta + \frac{1}{2}K_2\left[\frac{d\theta}{dx}\right]^2 \quad (1)$$

where F_A is the free energy of the undisturbed SmA*, χ is a generalized d.c. electric susceptibility, t is the piezoelectric coupling constant, and K_2 the twist elastic constant [3]. Since the layer thickness change associated with θ can be accommodated by tilt (see figure 9), equation (1) does not include a term describing the layer compression elasticity. The surface anchoring energy density, valid at $x = 0$ (where $\theta = \theta_s$), is given by

$$F_s = c\theta + \frac{1}{2}d\theta^2 \quad (2)$$

in which the terms describe respectively the polar and non-polar anchoring energies. By minimizing the total

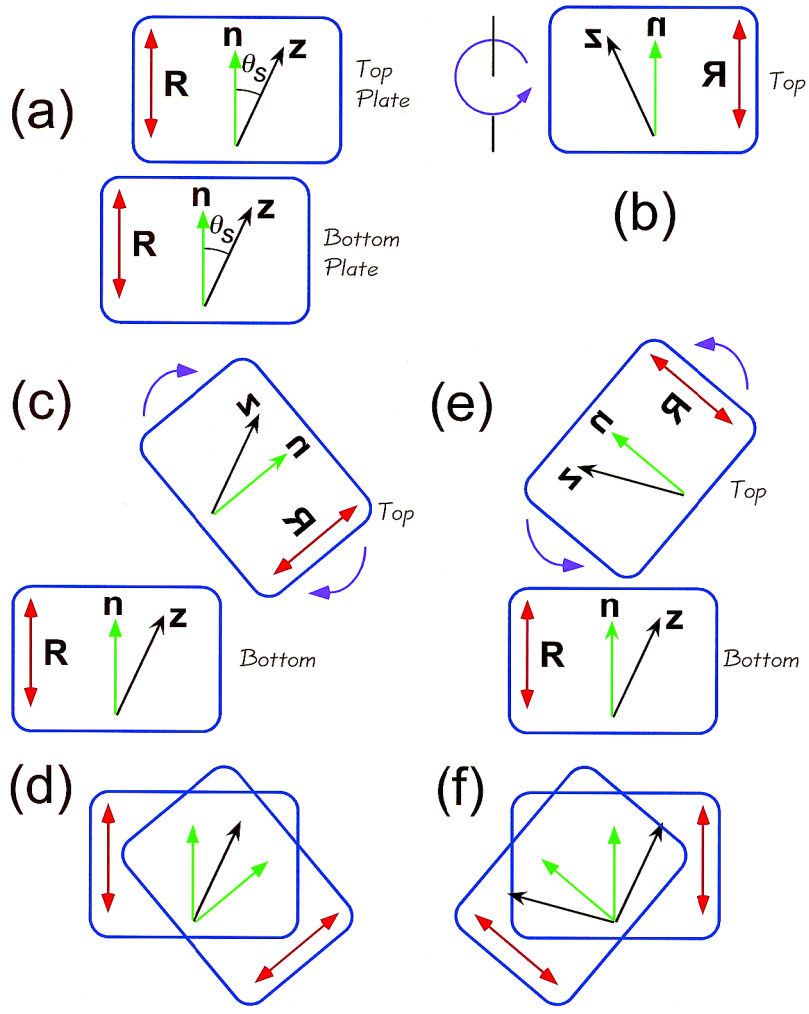

Figure 6. Assembling cross-rubbed surface electroclinic cells. The polymer-coated glass plates are rubbed identically (*a*) and the top plate is then flipped over (*b*). Relative rotation of the plates of the cell, (*c*) or (*e*), yields either parallel (*d*) or perpendicular (*f*) orientation of the layers growing in from the cell surfaces.

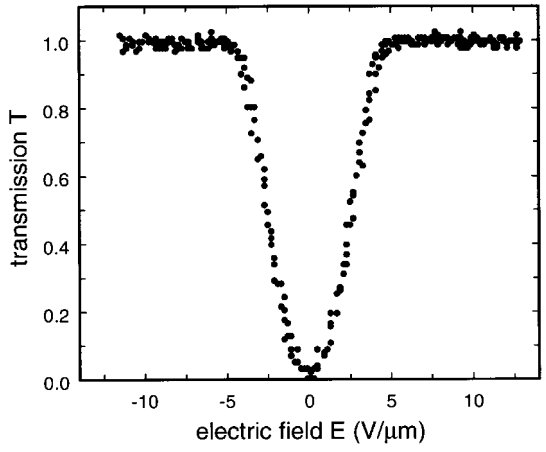

Figure 7. Linear ('V-shaped') electro-optic response $T(E)$ of a W415 cell cross-rubbed so that the layer orientation in the cell is uniform.

free energy, we obtain

$$P = \chi t\theta \tag{3 a}$$

$$\theta(x) = \theta_s \exp(-x/\xi) \tag{3 b}$$

where

$$\theta_s = c/(A\xi + d) \tag{4}$$

with $A = a(T - T_c)/T_c$ and $\xi = [K_2/(A - \chi t^2)]^{1/2}$. The correlation length is estimated in [3] to be $\xi \approx 1000/(T - T_c)^{1/2}$ Å in typical materials, where T_c is the SmA–SmC transition temperature.

Equation (4) predicts a large θ_s if the liquid crystal has a large polar interaction c with the surface, a small non-polar interaction d, and a small twist elastic constant K_2. Equation (4) also suggests that θ_s should depend

on temperature. Direct microscopic observation is not specifically sensitive to small changes in θ_s. According to our experiments, however, ψ is constant over a wide range of temperature, indicating that the smectic layer orientation is difficult to change at the surface once layers have formed at the isotropic–SmA transition. Since the polar surface interaction increases linearly with enantiomeric excess of W415 in the racemate, we would expect θ_s to increase linearly at low ee and saturate at high ee, just as in the bulk electroclinic effect [13].

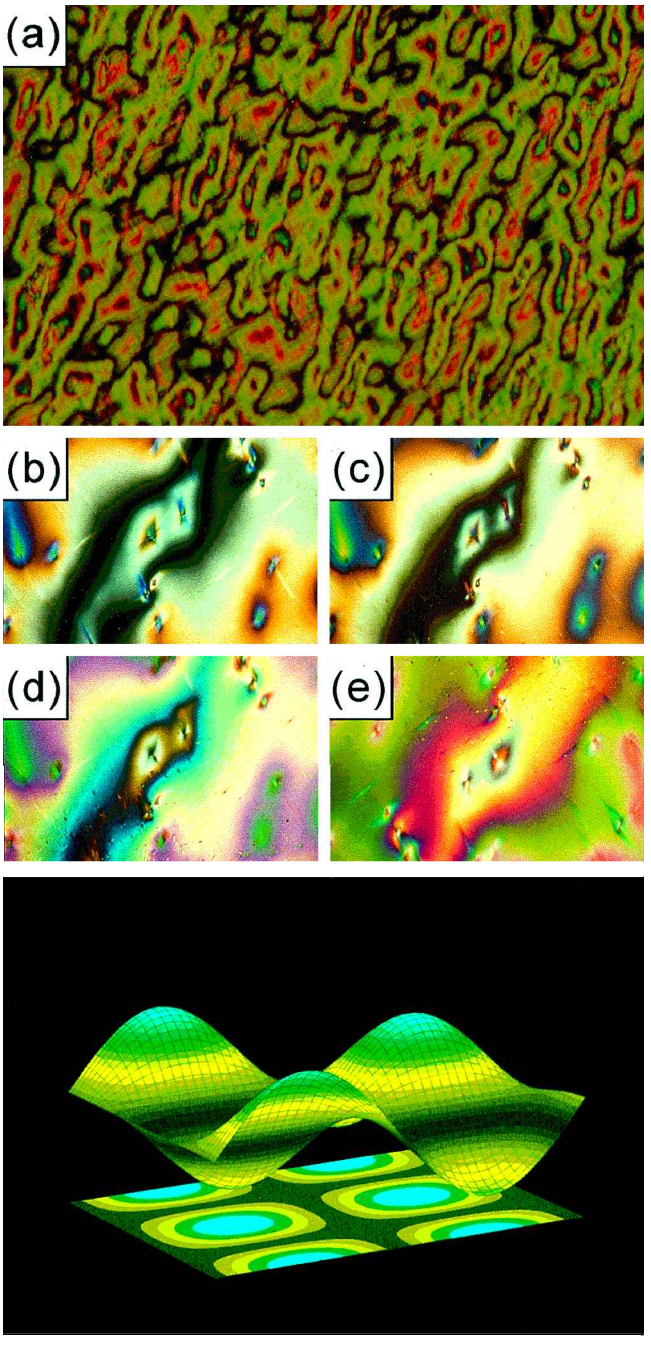

Figure 8. Texture of W415 cells ($d \sim 4\,\mu m$) cross-rubbed so that the smectic layers are orthogonal. (*a*) The black loops are contours of the internal layer interface where the net birefringence of the cell is zero. The pink and green regions on either side of each brush have the same effective birefringence but mutually orthogonal orientations of the optic axis (the polarizers are slightly decrossed). The horizontal dimension is about 200 µm. (*b*) Layer interface topography visualized between crossed polarizers and (*c*)–(*e*) progressively enhanced with a phase compensator orientated at 45° to the polarizers. The pale blue regions ('peaks') in (*b*) correspond to uniform layer orientation through most of the cell. Increasing the overall birefringence changes the extinction brush positions and emphasizes the contours of the internal layer interface. The birefringence colour sequences in the hills and valleys on either side of the black brushes also become increasingly different as the phase compensation is increased. The horizontal scale is the same as in (*a*). (*f*) Cartoon depicting the layer interface topography of these cells. The net birefringence, and hence the observed colour (bottom), depends on the position of the layer twist interface (top).

5. Director and layer structures

Measurements of the order parameter of LC monolayers on rubbed polyimide-coated substrates made using second-harmonic generation [5] confirm that the molecules lie nearly flat on the surface and have an average orientation parallel to the rubbing axis. The bulk is in the SmA* phase, with the molecular director normal to the layers. The thickness of the twisted interfacial region is of the order of $\xi_P = (K/4\pi P^2)^{1/2}$ [14]. If we assume for W415 an elastic constant $K = 4 \times 10^{-7}$ erg cm^{-1} and an induced polarization $P = 300$ nC cm^{-2}, we obtain $\xi_P \approx 0.05\,\mu m$.

The response of most FLC cells on cooling from the SmA* to the SmC* phase is that the layers adopt a chevron configuration [15], which allows the layer spacing to decrease with temperature without changing the molecular periodicity on the surfaces. The volume of each layer is constant.

Similarly, the change in layer thickness due to the surface electroclinic effect can also be compensated by deforming the layers. However, the resulting layer thickness is not spatially invariant as in the case of classical chevron cells, but changes as $d = d_1 \cos\theta(x)$ where $\theta(x) = \theta_s \exp(-x/\xi)$ and d_1 is the layer thickness of the bulk SmA* phase. Therefore the layer orientation changes continuously with distance from the surface and the layers are curved, as sketched in figure 9. Since the bulk and surface layer periodicities, d_1 and d_s, are not commensurate, the system presumably compensates by introducing periodic layer dislocations at the cell surface, spaced an estimated distance $d_1 d_s/(d_1 - d_s) \sim 10\,d_1$ apart.

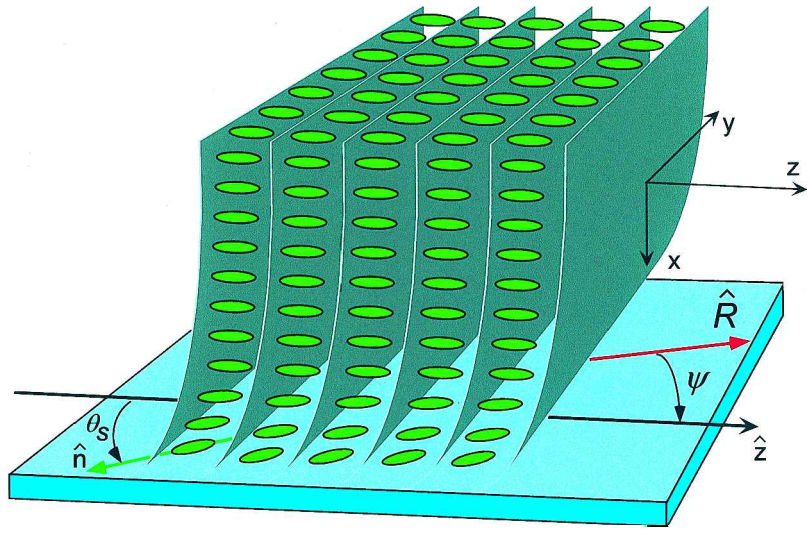

Figure 9. Layer-director structure of surface electroclinic SmA* cell. The surfaces induce a transition to the SmC* phase, with the director orientation twisting from along the rubbing direction at the surface to along the layer normal $\hat{z}$ in the bulk. The layer spacing decreases at the surface, causing layer curvature and necessitating the introduction of dislocations. The surface tilt θ_s here is negative, corresponding to the case of W415.

6. Conclusion

We have observed a giant surface electroclinic effect ($\theta_s \approx 24°$) in W415 and determined that the sign of the induced surface tilt depends on the molecular handedness. Appropriate cross-rubbing gives uniformly aligned samples that show 'V-shaped' electro-optic switching. However when the smectic layers grow in from the two plates with different orientations, the optical textures are non-uniform and the layering at the internal interface is accommodated by a new kind of focal-conic defect.

This work was supported by NSF MRSEC Grant DMR 98-09555, AFOSR MURI F49620-97-1-0014, and ARO Grant DAAG 55-98-10446.

References

[1] Nakagawa, K., Shinomiya, T., Koden, M., Tsubota, K., Kuratate, T., Ishii, Y., Funada, F., Matsuura, M., and Awane, K., 1988, *Ferroelectrics*, **85,** 39.

[2] Clark, N. A., and Lagerwall, S. T., 1980, *Appl. Phys. Lett.*, **36,** 899.

[3] Xue, J.-Z., and Clark, N. A., 1990, *Phys. Rev. Lett.*, **64,** 307.

[4] Patel, J. S., Lee, S.-D., and Goodby, J. W., 1991, *Phys. Rev. Lett.*, **66,** 1890.

[5] Chen, W., Ouchi, Y., Moses, T., Shen, Y. R., and Yang, K. H., 1992, *Phys. Rev. Lett.*, **68,** 1547.

[6] Li, Z., Petschek, R. G., and Rosenblatt, C., 1989, *Phys. Rev. Lett.*, **62,** 796; Li, Z., Petschek, P. G., and Rosenblatt, C., 1989, *Phys. Rev. Lett.*, **62,** 1557(E); Li, Z., DiLisi, G. A., Petschek, R. G., and Rosenblatt, C., 1990, *Phys. Rev. A*, **41,** 1997; Tripathi, S., Lu, M. H., Terentev, E. M., Petschek, R. G., and Rosenblatt, C., 1991, *Phys. Rev. Lett.*, **67,** 3400.

[7] Biradar, A. M., Bawa, S. S., Saxena, K., and Chandra, S., 1993, *J. Phys. II Fr.*, **3,** 1787.

[8] Kimura, M., Yamada, M., Ishihara, H., and Akahane, T., 1997, *Mol. Cryst. liq. Cryst.*, **302,** 199.

[9] Rudquist, P., Lagerwall, J. P. F., Buivydas, M., Gouda, F., Lagerwall, S. T., Clark, N. A., Maclennan, J. E., Shao, R., Coleman, D. A., Bardon, S., Bellini, T., Link, D. R., Natale, G., Glaser, M. A., Walba, D. M., Wand, M. D., and Chen, X.-H., 1999, *J. Mater. Chem.*, **9,** 1257.

[10] Clark, N. A., Coleman, D., and Maclennan, J. E., (to be published).

[11] Garoff, S., and Meyer, R. B., 1977, *Phys. Rev. Lett.*, **38,** 848; Garoff, S., and Meyer, R. B., 1979, *Phys. Rev. A*, **19,** 338.

[12] Gießelmann, F., and Zugenmaier, P., 1995, *Phys. Rev. E*, **52,** 1762.

[13] Andersson, G., Dahl, I., Komitov, L., Lagerwall, S. T., Skarp, K., and Stebler, B., 1989, *J. Appl. Phys.*, **66,** 4983.

[14] Zhuang, Z., Maclennan, J. E., and Clark, N. A., 1989, *Proc. SPIE*, **1080,** 110.

[15] Rieker, T. P., Clark, N. A., Smith, G. S., Parmar, D. S., Sirota, E. B., and Safinya, C. R., 1988, *Phys. Rev. Lett.*, **59,** 2658; Clark, N. A., and Rieker, T. P., 1988, *Phys. Rev. A*, **37,** 1053.